Published in final edited form as:

Nature. 2010 December 9; 468(7325): 779–783. doi:10.1038/nature09605.

Cap binding and immune evasion revealed by Lassa nucleoprotein structure

Xiaoxuan Qi[1], **Shuiyun Lan**[2], **Wenjian Wang**[3], **Lisa McLay Schelde**[2], **Haohao Dong**[1], **Gregor D. Wallat**[1], **Hinh Ly**[2,*], **Yuying Liang**[2,*], and **Changjiang Dong**[1,*]

[1]Biomedical Sciences Research Complex, School of Chemistry, University of St. Andrews, North Haugh, St. Andrews, Fife KY16 9ST, UK

[2]Department of Pathology and Laboratory Medicine, Emory University School of Medicine, 615 Michael St., Atlanta, Georgia 30322, USA

[3]Laboratory of Department of Surgery, The First Affiliated Hospital, Sun Yat-Sen University, 58 Zhongshan Road II, Guangzhou, Guangdong 510080, China

Summary

Lassa fever virus (LASV) causes thousands of deaths yearly and is a biological threat agent, for which there is no vaccine and limited therapy1. The nucleoprotein (NP) of LASV plays essential roles in viral RNA synthesis and immune suppression2-6, the molecular mechanisms of which are poorly understood. Here, we report the crystal structure of LASV NP at 1.80 Angstrom resolution, which reveals N- and C-domains with structures unlike any of the reported viral NPs7-10. The N domain folds into a novel structure with a deep cavity for binding the m7GpppN cap structure that is required for viral RNA transcription, whereas the C domain contains 3′-5′ exoribonuclease activity involved in suppressing interferon induction. This is the first X-ray crystal structure solved for an arenaviral NP, which reveals its unexpected functions and suggests unique mechanisms in cap binding and immune evasion. These findings provide great potential for vaccine and drug development.

Several arenaviruses including LASV can cause severe viral haemorrhagic fevers in humans with high morbidity and mortality, to which there is no vaccine and limited treatments 1,11-13. These pathogenic arenaviruses are public health threats and potential biological threat agents. LASV, like other arenaviruses, is a single-stranded ambisense RNA virus with two genomic RNA segments encoding four genes1. The NP encapsidates viral genomic

*Correspondence should be addressed to: CJD (cd26@st-and.ac.uk), YL (yliang5@emory.edu), or HL (hly@emory.edu).

Author contributions: XQ, SL, WW, LMS, HD, GW performed experiments. CJD, YL and HL conceived the idea for the study, performed some of the assays, participated in the analysis and interpretation of the data, and wrote the manuscript. All authors contributed to the final version of the manuscript.

Author information: atomic coordinates and structure factors for the structures have been deposited in the Protein Data Bank under the accession codes 3MWP for the native, 3MWT for the manganese complex, 3MX2 for the dTTP complex and 3MX5 for the UTP complex. Reprints and permissions information is available at www.nature.com/reprints.

Supplementary information is linked to the online version of the paper at www.nature.com/nature

Full Methods and references are available in the online version of the paper at www.nature.com/nature.

The authors declare no competing financial interests.

RNAs into ribonucleoprotein (RNP) complexes and is required for both RNA replication and transcription2-4. Like bunyaviruses and orthomyxoviruses, arenaviruses snatch the cap structure of cellular mRNAs to use as primers to initiate viral transcription, the exact mechanism of which is unknown. The cap snatching mechanism of arenaviruses seems to be unique, as evidenced by the cytoplasmic localization and the much shorter 5′ nontemplated mRNA sequences14-17. Severe arenavirus infections including lethal Lassa cases are associated with a generalised immune suppression in the infected hosts18-24, the exact mechanism of which is unclear but is thought to involve NP's ability to suppress the induction of type I IFN5,6. To address the functional mechanisms of NP in viral RNA synthesis and host immune suppression, we set out to determine the crystal structure for LASV NP, knowledge derived from which can be extended to other arenavirus NP proteins, as all known arenaviral NP proteins share high sequence identity (Supplementary Fig. S1).

Structure determination

The full-length 569-residue LASV NP protein (Josiah strain) was expressed and purified as a recombinant MBP fusion protein in *E. coli* as described in Methods. The purified protein exists mainly in two forms, with a majority in trimeric and some in hexameric form. Both forms bind random RNAs, which are longer and more abundant in the hexamers than in the trimers, a feature that is similar to known NPs from negative-strand RNA viruses7-10. We attempted to crystallise both forms, but only the trimeric NP formed crystals. The crystals showed heavy twining with a twin fraction of ~0.43 and $[E^2-1]$ 0.681/0.681. Initial phases were obtained in a space group of P321 using the Multiple wavelength Anomalous Diffraction (MAD) with Samarium derivative. The true space group was P3 with three subunits in an asymmetric unit. The structure was refined to a resolution of 1.80 Angstrom (Å) with detwining. The crystal structures do not contain RNA, indicating that only RNA-free NP was able to form crystals. The final structural model of the native LASV NP has an R_{factor} of 0.18 and an R_{free} of 0.20. Data collection, phasing, and refinement statistics are provided in Supplementary Table S1.

Overall structure of LASV NP protein

In the NP protomer structure, 514 residues of the 569-residue LASV NP protein were built into the model (Fig. 1a). The electron densities for residues 1 to 6, 147 to 157, 339 to 363, 518 to 521, 562 to 569 were not well defined. LASV NP protomer, like other viral NPs7-10, is composed of the N- and the C-terminal domains (Fig. 1a), but neither domain shows structure similarity to any known viral NPs (Supplementary Table S2). The large N domain (residues 7 to 338) consists mainly of alpha helices and coils, while the C domain (residues 364 to 561) forms a typical α/β/α sandwich architecture (Fig.1a and Supplementary Text S1). Surface rendering reveals a deep cavity located near the bottom of the N domain and a large cavity at the top of the C domain (Fig. 1c and 1d), which are the cap-binding site and the 3′ to 5′ exoribonuclease active site (see below), respectively. In the trimeric form, three subunits lie in a head-to-tail orientation to form a ring-shaped structure with a three-fold symmetry (Fig. 1b and Supplementary Fig.S2). The interface area between the subunits is 455 $Å^2$, representing 1.9 % of total surface area of a subunit (23343 $Å^2$). The central hole of

the trimeric structure is 23 Å in diameter, while the head ring is 98 Å and the body ring is 118 Å (Supplementary Fig.S2).

LASV NP is a 3′-5′ exoribonuclease

A Dali search (http://ekhidna.biocenter.helsinki.fi/dali_server) identified several structures similar to the C domain of NP, including several known 3′ to 5′ exonucleases/ exoribonucleases in bacteria and humans (e.g., human TREX1) (Supplementary Text S2), all of which belong to the DEDDH subfamily of the DEDD (DnaQ) superfamily25-27. The human TREX1 structure shows two Mn^{2+} cations in the active site27. We identified one Mn^{2+} in each subunit of LASV NP by crystal fluorescent scanning, but could not identify the second Mn^{2+}, possibly because it was not well ordered in the absence of the RNA substrate. The C domain of NP superimposes well with the portion of TREX1 that coordinates the Mn^{2+} cations (Fig. 2a), in particular the β5, β6, β7, β8 and β9 strands of NP completely overlap with the central β sheets of TREX1. The putative exonuclease catalytic residues D389, E391, D466, D533 and H528 are absolutely conserved in all known arenavirus NP proteins and are located at identical positions as in the TREX1 active cavity (Fig. 2b). Taken together, the structural evidence suggests that LASV NP is a new member of the DEDD 3′-5′ exonuclease superfamily.

We conducted in vitro assays to characterise the 3′- 5′ exonuclease activity of the wild-type (WT) LASV NP, as well as NP mutants at putative catalytic sites. We showed that the WT protein, in its trimeric or hexameric form, could digest both DNA and RNA substrates (Supplementary Figs. S3 and S4). As divalent cations are essential for exonuclease activity25, we determined what divalent cation was most effective for NP exonuclease to digest various single-stranded RNA (ssRNA) species that are based on the NP gene in either viral genomic sense (60 nts, vRNA), complementary antigenomic sense (30 nts, cRNA), or in capped mRNA form (126 nts, mRNA) (Methods). We showed the order of efficiency as Mn^{2+} >Co^{2+}> Mg^{2+} >Ca^{2+} >Zn^{2+} >Fe^{2+}>Ni^{2+}>Cu^{2+} (Supplementary Fig. S5). WT NP could cleave various ssRNA species efficiently (Fig. 2c), regardless of whether they contained a hydroxyl (5′OH) group, triphosphate (5′ppp), or a cap at the 5′ termini (Methods). In contrast, the NP catalytic mutants (D389A, E391A, and D466A) showed markedly reduced ribonuclease activity (Fig. 2c and Supplementary Fig. S4). In addition, we showed that WT NP, but not its catalytic mutants, could digest cellular RNA substrates in vitro with a preference toward short RNA species over long ones (e.g., 18s rRNA vs. β-globin mRNA, the large vs. small fragments in the RNA ladder) (Supplementary Figs. S6 and S7).

Fluorescence scanning analysis identified a zinc ion in the NP structure, despite the fact that no typical zinc finger motif was predicted from the amino acid sequence and that no zinc compounds were used during the purification and crystallisation processes. Although the residues C506, C529, H509 and E399 that coordinate the zinc ion are not of the typical zinc-binding motif28, they appear to adopt a zinc finger fold in structure28,29. The CCHE zinc-binding site is located in the C domain near the 3′-5′ exonuclease active site (Supplementary Fig. S8). We speculate that zinc binding may be required to stabilise the structure of the C domain and/or contribute to the substrate binding and specificity of the exonuclease

activity28,29. A highly positively-charged groove located between the N- and C-domains is predicted as the genomic RNA-binding site (Supplementary Fig. S9). In vitro assay confirmed that RNAs are bound within the purified NP oligomers and protected from its intrinsic exonuclease activity (Supplementary Figs.S9, S10, Text S3 and method S1).

Exonuclease and immune evasion

To determine whether the exoribonuclease activity is important for the transcriptional function of NP, we generated alanine substitution at five putative catalytic sites, D389A, E391A, D466A, D533A and H528A, in the mammalian cell expression vectors of either native or myc-tagged NP gene, and examined the activity of each mutant in transcribing the LASV mini-genome RNA that encodes a renilla luciferase (RLuc) reporter gene6 (Methods). As shown in Fig. 3a, each NP mutant expressed comparable protein levels to the WT, and led to similar folds of increase in RLuc activity, suggesting that these mutations did not alter the overall structure (Supplementary Text S4 and Supplementary Fig. S11) or affect the basic function of NP in mediating viral RNA transcription.

We next examined whether the exoribonuclease activity is required for NP's function in the IFN suppression5,6. As expected, WT NP strongly inhibited Sendai virus-induced IFN-beta activation by a promoter assay (Methods), whereas all the catalytic mutants D389A, E391A, D466A, D533A, and H528A showed a complete loss of function at a low level of transfected expression vectors (10 ng) and showed various levels of deficiency at higher levels (Fig. 3b and Supplementary Fig. S12). Our results confirm a previous study showing that the D389 residue of LASV NP, as well as its corresponding residue D382 in the prototypic arenavirus lymphocytic choriomeningitis virus (LCMV), is required for the IFN suppression but not for viral RNA transcription30, and may help to explain the loss of IFN suppression for Tacaribe virus NP (Supplementary Fig S13, and Text S5). In summary, these data provide strong genetic evidence for an important role of the NP exoribonuclease activity in suppressing the IFN induction.

Viral infections are usually detected by the cellular pattern-recognition receptors (PRRs) such as toll-like receptors (TLRs) and cytosolic RNA sensors, retinoid acid-inducible gene-I-like helicase (RIG-I) and melanoma differentiation-associated protein 5 (MDA-5), which recognise the pathogen-associated molecular patterns (PAMP) RNA ligands and initiate signalling pathways to induce the production of type I IFNs 31,32. We hypothesise that NP prevents the virus-induced IFN induction by degrading the PAMP RNA ligands that otherwise would trigger the viral sensors in the cells. We show that WT NP, but not its catalytic mutants (D389A, E391A, and D466A), can efficiently degrade different ssRNA substrates (Fig. 2c) and various dsRNA molecules with 5′-hydroxyl (5′-OH), single 5′-triphosphorylate (5′-ppp/5′-OH), and double 5′-triphosphorylate (5′-ppp/5′-ppp), as well as long dsRNA mimics poly(I:C) (Figs. 2d and Supplementary Fig. S14).

We examined whether the NP ribonuclease function is essential for suppressing the IFN production induced by the immunostimulatory RNAs, i.e., poly(I:C) and the virion RNAs extracted from Pichinde virus, which is a prototypic arenavirus33. We found that whereas WT NP efficiently inhibited the IFN-beta activation induced by poly(I:C) or by Pichinde

virion-associated RNAs, none of the 5 catalytic mutants (D389A, E391A, D466A, D533A, and H528A) exhibited any suppressive activity (Fig. 3c). Similar results had been reported for LCMV NP 34.

In summary, we have shown that the NP exoribonuclease activity is essential for suppressing both viral infection-induced and immunostimulatory RNAs-induced IFN production. A good example of the exonuclease function in suppressing the IFN production has been demonstrated for human TREX1 protein, which degrades small ssDNAs and dsDNAs accumulated during cellular apoptosis. Failure to clear these DNA fragments by TREX1 natural mutants lead to the activation of cellular DNA receptors to trigger a persistent production of IFNs that contribute to human autoimmune diseases27,35-38. How does the NP ribonuclease activity function in suppressing the virus-induced IFN production? A simplistic but reasonable model is that the NP ribonuclease activity is able to remove viral PAMP RNAs that are otherwise recognised by the cellular PRRs. Although we have shown that LASV NP protein can degrade various RNA templates in vitro, we believe that the NP ribonuclease activity must be highly regulated in vivo, as NP does not cause a generalised non-specific RNA degradation process of cellular or viral RNAs in the cells (Supplementary text S6 and Fig. S15). We propose that the NP ribonuclease activity in the cells is restricted to viral PAMP RNAs through a yet-to-be characterised regulatory mechanism. A recent publication has shown a direct protein-protein interaction of NP with RIG-I and MDA534, which may be one possible mechanism for the specific nuclease activity of NP against these PRRs-associated PAMP RNAs.

LASV NP is a cap binding protein

The N domain adopts a completely novel fold not found in the Dali server. In order to identify the cap-binding residues in the deep cavity of the N domain, we attempted to soak and perform co-crystallization of LASV NP with m7GpppG, triphosphorylated, diphosphorylated or monophosphorylated ribonucleotides (Methods). We could observe the clear density for the triphosphate and partial density for uridine (Supplementary Fig. S16) from the triphosphorylated ribonucleotide complex structures. We also visualized the structure of NP in complex with dTTP with a clear original Fo-Fc electron density contoured at 2.5 σ for dTTP (Fig. 4a). The triphosphate group of dTTP was bound in the middle of the cavity in an identical manner as that of UTP (Supplementary Fig. S16), in which it was anchored by salt bonds formed with the side chains of the conserved residues K309, R300, R323, and K253 (Fig. 4a). In the deep end of the cavity, thymidine occupied a hydrophobic pocket that is composed of residues F176, W164, L172, M54, L120, L239, and I241. We propose that this dTTP-binding pocket is the binding site for the cap structure m7GTP and that the residues located within the pocket may have to change conformation in order to accommodate the cap moiety. Although the N domain of NP is not structurally similar to any of the cap-binding proteins (Supplementary Table S3), its hydrophobic thymidine-binding pocket shares common features for cap binding39,40. Moreover, the NP cap-binding cavity has a unique feature in that its entrance contains another hydrophobic region that is composed of the hydrophobic residues Y319, Y209, Y213, L265 and the acidic residue E266, which can potentially act as the binding site for the second base of the m7GpppN (N represents G, C, U or A) cap structure. The entrance of the cap-binding cavity

has an oval shape with a diameter of 9 - 13 Å, which is a perfect fit for the single-stranded mRNA. We propose that a loop composed of residues K236 to S242 serves as a “gate” for the capped template (primer) binding and that the entire structure of m7GpppN, including the cap m7G, the triphosphate, and at least one more nucleotide, is embedded within the deep cavity. This binding feature is unlike other known cap-binding proteins, in which only the m7G caps are locked in between the sandwich, while the rest of the molecules is exposed39,40.

To characterize the role of the cap-binding residues in viral RNA transcription, we examined a panel of NP mutants with alanine substitution of residues located inside and at the entrance of the cavity and are conserved among all known arenaviruses for their ability to mediate the cap-dependent viral RNA transcription using the LASV mini-genome replicon assay (Methods). WT NP (with or without myc tag) produced up to 1000 fold increase in RLuc reporter activity over a control reaction, and more than 100 fold increase even when expressed at a low level (15 ng of transfected NP plasmid DNAs) (Figure 4c). All mutant proteins were expressed at similar levels as the WT transfected with 15 to 30 ng of plasmid (Fig. 4b). Compared to the WT, the K253A and E266A mutants completely lost the RNA transcription activity, and the Y319A, F176A, W164A, K309A, and R323A mutants showed significantly decreased activity (Fig. 4c). R300A had a minor effect, while W12A and Y209A had no effect (Fig. 4c). It is worth noting that none of these mutants was found to impact the NP function in the IFN suppression (Supplementary Fig. S17). These functional data correlate well with the proposed cap-binding function of some of these conserved residues.

The unique cap-binding feature of LASV NP in that the entire cap structure m7GpppN is buried within the cavity has significant implications in understanding the distinctive cap snatching mechanism of arenaviruses. Once NP binds and protects the 5′ cap m7GpppN, the rest of mRNA molecule located outside of the cavity may be susceptible to viral and/or host exonuclease-mediated degradation and/or to endonuclease-mediated cleavage (Supplementary Fig. S9). This may help explain the relatively short (1-4 nt) 5′ non-templated sequences in arenavirus mRNAs1,14,15. However, individual mutation of the NP exonuclease catalytic sites did not show any defect in viral cap-dependent RNA transcription (Fig. 3a), suggesting that the NP exonuclease activity is not essential (required) for generating the capped primers. It is worth noting that we did not identify an influenza PA-like endonuclease structural motif 41,42 within LASV NP structure (Supplementary Table S4). Instead, recent studies suggested that LASV L polymerase protein contains an endonuclease domain in its N terminus that is crucial for the cap-dependent viral RNA transcription43,44.

Conclusion

Our structural analysis and functional assays have demonstrated that the C domain of LASV NP contains 3′-5′ exoribonuclease activity that is required for suppressing the IFN-beta induction. We have provided evidence to suggest that the NP ribonuclease activity is highly regulated in the cells and proposed a novel mechanism by which the NP ribonuclease activity may specifically remove the viral PAMP RNA ligands in order to suppress the IFN

production. Another important feature of LASV NP protein is that its N domain contains a deep cavity to bind and shield the entire m7GpppN cap structure, which is distinct from other known cap-binding proteins, and has shed important lights on the unique cap-snatching mechanism of arenaviruses. In addition, we have also identified an unusual zinc-binding site and the viral RNA-binding groove in the LASV NP structure. Taken together, these novel findings reveal several new and potentially vulnerable targets on NP for the development of antivirals and effective vaccines to combat LASV and other pathogenic arenaviruses that can cause severe hemorrhagic fever diseases in humans.

Method Summary

The crystals were grown using the sitting drop, and the native structure was determined with the MAD data. All the NP mutations were generated using QuickChange site-directed mutagenesis kit (Stratagene) and confirmed by DNA sequencing. The RNA synthesis assays used the LASV mini-genome (MG) system, and the Sendai virus-induced IFN-beta activation assay was conducted as described 45. The immunostimulatory RNAs-induced IFN-beta activation assay was conducted by transfecting HEK293 cells with the IFNbeta-LUC promoter construct and either WT or mutant NP construct, followed by Lipofectamine 2000-mediated transfection of poly(I:C) or Pichinde virion-isolated RNAs. Activation of the IFNbeta promoter was quantified by measuring the LUC activity.

Supplementary Material

Refer to Web version on PubMed Central for supplementary material.

Acknowledgements

CJD wishes to thank Prof. James Naismith for his continuing support, encouragement and invaluable advice, Prof. Richard M. Elliott for providing the human beta-globin containing plasmid phRL-CMV and his critical reading of the manuscript, Dr. Huanting Liu for discussions and Dr. Louise Major for the pLou3 plasmid. CJD is a Wellcome trust career development fellow (083501/Z/07/Z). We thank the staffs at IO2 and IO3 beam stations of Diamond light sources for their assistance of data collection. This work was supported in part by funds from the Southeast Regional Center of Excellence for Emerging Infections and Biodefense (5-U54-AI-057157-06), the pilot component of the U19 grant (5-U19-AI057266-07), and the Emory University Research Committee (URC) to YL and HL, a seed grant from the Emory DDRDC (DK64399) and a research scholar grant from the American Cancer Society (RSG-06-162-01-GMC) to HL, NIH grant R01AI083409 to YL, and NIH grant AI067704 to T.G. Parslow and YL. We thank Drs. K. Curtis and T.W. Geisbert for providing us with non-infectious genomic RNA samples of LASV and Dr. J. Aronson for the PICV virus.

References

1. Buchmeier, MJ.; De La Torre, JC.; Peters, CJ. Fields Virology. Knipe, DM.; Howley, PM., editors. Vol. 2. Lippincott Williams & Wilkins; 2007. p. 1791-1827.
2. Hass M, Golnitz U, Muller S, Becker-Ziaja B, Gunther S. Replicon system for Lassa virus. J Virol. 2004; 78:13793–13803. [PubMed: 15564487]
3. Pinschewer DD, Perez M, de la Torre JC. Role of the virus nucleoprotein in the regulation of lymphocytic choriomeningitis virus transcription and RNA replication. J Virol. 2003; 77:3882–3887. [PubMed: 12610166]
4. Lopez N, Jacamo R, Franze-Fernandez MT. Transcription and RNA replication of tacaribe virus genome and antigenome analogs require N and L proteins: Z protein is an inhibitor of these processes. J Virol. 2001; 75:12241–12251. [PubMed: 11711615]

5. Martinez-Sobrido L, Giannakas P, Cubitt B, Garcia-Sastre A, de la Torre JC. Differential inhibition of type I interferon induction by arenavirus nucleoproteins. J Virol. 2007; 81:12696–12703. [PubMed: 17804508]
6. Martinez-Sobrido L, Zuniga EI, Rosario D, Garcia-Sastre A, de la Torre JC. Inhibition of the type I interferon response by the nucleoprotein of the prototypic arenavirus lymphocytic choriomeningitis virus. J Virol. 2006; 80:9192–9199. [PubMed: 16940530]
7. Green TJ, Zhang X, Wertz GW, Luo M. Structure of the vesicular stomatitis virus nucleoprotein-RNA complex. Science. 2006; 313:357–360. [PubMed: 16778022]
8. Tawar RG, et al. Crystal structure of a nucleocapsid-like nucleoprotein-RNA complex of respiratory syncytial virus. Science. 2009; 326:1279–1283. [PubMed: 19965480]
9. Ye Q, Krug RM, Tao YJ. The mechanism by which influenza A virus nucleoprotein forms oligomers and binds RNA. Nature. 2006; 444:1078–1082. [PubMed: 17151603]
10. Albertini AA, et al. Crystal structure of the rabies virus nucleoprotein-RNA complex. Science. 2006; 313:360–363. [PubMed: 16778023]
11. Delgado S, et al. Chapare virus, a newly discovered arenavirus isolated from a fatal hemorrhagic fever case in Bolivia. PLoS Pathog. 2008; 4:e1000047. [PubMed: 18421377]
12. Briese T, et al. Genetic detection and characterization of Lujo virus, a new hemorrhagic fever-associated arenavirus from southern Africa. PLoS Pathog. 2009; 5:e1000455. [PubMed: 19478873]
13. Khan SH, et al. New opportunities for field research on the pathogenesis and treatment of Lassa fever. Antiviral Res. 2008; 78:103–115. [PubMed: 18241935]
14. Polyak SJ, Zheng S, Harnish DG. 5′ termini of Pichinde arenavirus S RNAs and mRNAs contain nontemplated nucleotides. J Virol. 1995; 69:3211–3215. [PubMed: 7707553]
15. Meyer BJ, Southern PJ. Concurrent sequence analysis of 5′ and 3′ RNA termini by intramolecular circularization reveals 5′ nontemplated bases and 3′ terminal heterogeneity for lymphocytic choriomeningitis virus mRNAs. J Virol. 1993; 67:2621–2627. [PubMed: 7682625]
16. Jin H, Elliott RM. Characterization of Bunyamwera virus S RNA that is transcribed and replicated by the L protein expressed from recombinant vaccinia virus. J Virol. 1993; 67:1396–1404. [PubMed: 8437222]
17. Plotch SJ, Bouloy M, Ulmanen I, Krug RM. A unique cap(m7GpppXm)-dependent influenza virion endonuclease cleaves capped RNAs to generate the primers that initiate viral RNA transcription. Cell. 1981; 23:847–858. [PubMed: 6261960]
18. Edington GM, White HA. The pathology of Lassa fever. Trans R Soc Trop Med Hyg. 1972; 66:381–389. [PubMed: 5046378]
19. Fisher-Hoch S, McCormick JB, Sasso D, Craven RB. Hematologic dysfunction in Lassa fever. J Med Virol. 1988; 26:127–135. [PubMed: 3183637]
20. McCormick JB, Fisher-Hoch SP. Lassa fever. Curr Top Microbiol Immunol. 2002; 262:75–109. [PubMed: 11987809]
21. Baize S, et al. Early and strong immune responses are associated with control of viral replication and recovery in lassa virus-infected cynomolgus monkeys. J Virol. 2009; 83:5890–5903. [PubMed: 19297492]
22. Baize S, et al. Lassa virus infection of human dendritic cells and macrophages is productive but fails to activate cells. J Immunol. 2004; 172:2861–2869. [PubMed: 14978087]
23. Mahanty S, et al. Cutting edge: impairment of dendritic cells and adaptive immunity by Ebola and Lassa viruses. J Immunol. 2003; 170:2797–2801. [PubMed: 12626527]
24. Muller S, Geffers R, Gunther S. Analysis of gene expression in Lassa virus-infected HuH-7 cells. J Gen Virol. 2007; 88:1568–1575. [PubMed: 17412988]
25. Cisneros GA, et al. Reaction mechanism of the epsilon subunit of E. coli DNA polymerase III: insights into active site metal coordination and catalytically significant residues. J Am Chem Soc. 2009; 131:1550–1556. [PubMed: 19119875]
26. Zuo Y, et al. Crystal structure of RNase T, an exoribonuclease involved in tRNA maturation and end turnover. Structure. 2007; 15:417–428. [PubMed: 17437714]

27. de Silva U, et al. The crystal structure of TREX1 explains the 3′ nucleotide specificity and reveals a polyproline II helix for protein partnering. J Biol Chem. 2007; 282:10537–10543. [PubMed: 17293595]
28. Hall TM. Multiple modes of RNA recognition by zinc finger proteins. Curr Opin Struct Biol. 2005; 15:367–373. [PubMed: 15963892]
29. Matthews JM, Sunde M. Zinc fingers--folds for many occasions. IUBMB Life. 2002; 54:351–355. [PubMed: 12665246]
30. Martinez-Sobrido L, et al. Identification of amino acid residues critical for the anti-interferon activity of the nucleoprotein of the prototypic arenavirus lymphocytic choriomeningitis virus. J Virol. 2009; 83:11330–11340. [PubMed: 19710144]
31. Kawai T, Akira S. Innate immune recognition of viral infection. Nat Immunol. 2006; 7:131–137. [PubMed: 16424890]
32. McCartney SA, Colonna M. Viral sensors: diversity in pathogen recognition. Immunol Rev. 2009; 227:87–94. [PubMed: 19120478]
33. Lan S, et al. Development of infectious clones for virulent and avirulent pichinde viruses: a model virus to study arenavirus-induced hemorrhagic fevers. J Virol. 2009; 83:6357–6362. [PubMed: 19386714]
34. Zhou S, et al. Induction and inhibition of type I interferon responses by distinct components of lymphocytic choriomeningitis virus. J Virol. 2010; 84:9452–9462. [PubMed: 20592086]
35. Crow YJ, Rehwinkel J. Aicardi-Goutieres syndrome and related phenotypes: linking nucleic acid metabolism with autoimmunity. Hum Mol Genet. 2009; 18:R130–136. [PubMed: 19808788]
36. Lee-Kirsch MA, et al. Mutations in the gene encoding the 3′-5′ DNA exonuclease TREX1 are associated with systemic lupus erythematosus. Nat Genet. 2007; 39:1065–1067. [PubMed: 17660818]
37. Lehtinen DA, Harvey S, Mulcahy MJ, Hollis T, Perrino FW. The TREX1 double-stranded DNA degradation activity is defective in dominant mutations associated with autoimmune disease. J Biol Chem. 2008; 283:31649–31656. [PubMed: 18805785]
38. Stetson DB, Ko JS, Heidmann T, Medzhitov R. Trex1 prevents cell-intrinsic initiation of autoimmunity. Cell. 2008; 134:587–598. [PubMed: 18724932]
39. Guilligay D, et al. The structural basis for cap binding by influenza virus polymerase subunit PB2. Nat Struct Mol Biol. 2008; 15:500–506. [PubMed: 18454157]
40. Fechter P, Brownlee GG. Recognition of mRNA cap structures by viral and cellular proteins. J Gen Virol. 2005; 86:1239–1249. [PubMed: 15831934]
41. Yuan P, et al. Crystal structure of an avian influenza polymerase PA(N) reveals an endonuclease active site. Nature. 2009; 458:909–913. [PubMed: 19194458]
42. Dias A, et al. The cap-snatching endonuclease of influenza virus polymerase resides in the PA subunit. Nature. 2009; 458:914–918. [PubMed: 19194459]
43. Lelke M, Brunotte L, Busch C, Gunther S. An N-terminal region of Lassa virus L protein plays a critical role in transcription but not replication of the virus genome. J Virol. 2010; 84:1934–1944. [PubMed: 20007273]
44. Morin B, et al. The N-terminal domain of the arenavirus L protein is an RNA endonuclease essential in mRNA transcription. PLoS Pathog. 2010; 6:e1001038. [PubMed: 20862324]
45. Lan S, McLay L, Aronson J, Ly H, Liang Y. Genome comparison of virulent and avirulent strains of the Pichinde arenavirus. Arch Virol. 2008; 153:1241–1250. [PubMed: 18506572]

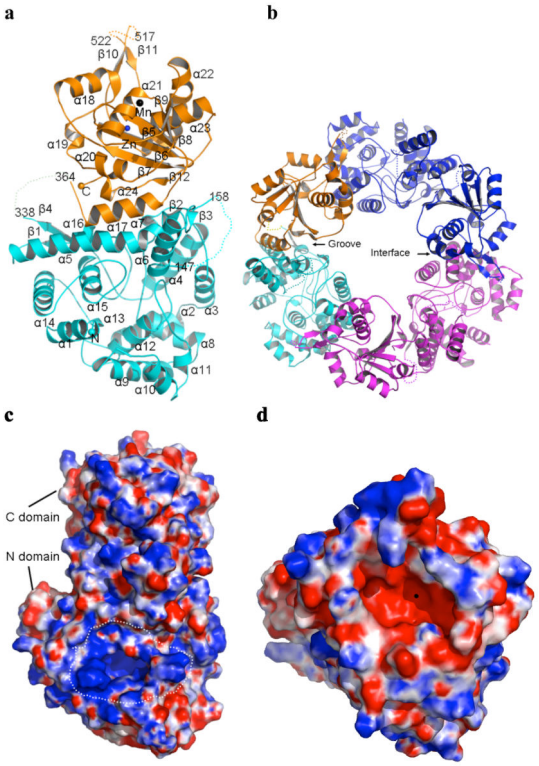

Figure 1. The crystal structure of LASV NP protein

a, Cartoon diagram of the LASV NP protomer. N domain in cyan with cyan sphere indicating the N terminus, C domain in orange with orange sphere indicating the C terminus. Black sphere shows Mn^{2+}, while blue sphere shows Zn^{2+}. The dotted lines represent the disordered loops. **b**, The ring-shaped structure of LASV NP trimer. The first protomer coloured as in (a), the second protomer in blue and the third in magenta. The groove and the interface are indicated by arrows. **c**, Electrostatic surface potential map of the NP protomer. The entrance of the cap-binding cavity shown as white dotted circle. The blue area represents positively charged residues and the red area represents negatively charged residues. **d**, Electrostatic surface potential map of the 3′-5′ exoribonuclease cavity. The black sphere represents Mn^{2+}.

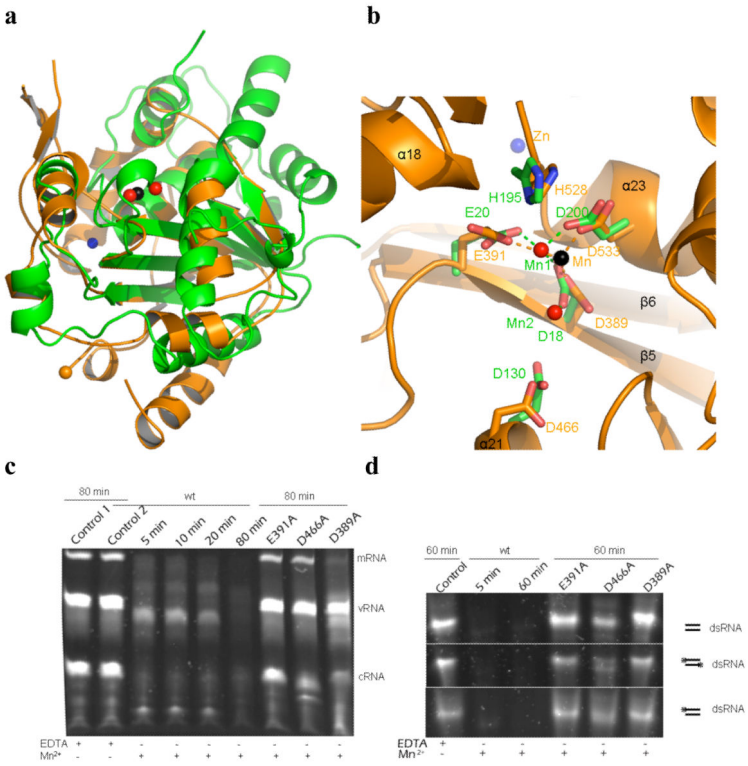

Figure 2. The C domain of LASV NP protein is a 3′-5′ exoribonuclease

a, Superimposition of the C domain (orange) with human TREX1 protein (green) reveals a high degree of similarity between the two structures.The Mn^{2+} in black in LASV NP and in red in TREX1, the Zn^{2+} in blue. **b**, The exonuclease catalytic residues of LASV NP and TREX1 are located to identical positions, and shown in orange for NP and in green for TREX1. **c**, The exoribonuclease activities of the WT and mutant LASV NP with different ssRNAs as substrates. Control 1 contains 10 mM EDTA and no NP. Control 2 contains 10 mM EDTA and NP. **d**, Comparison of the WT and NP catalytic mutants in degrading the dsRNA substrates, the 5′-hydroxyl dsRNA (upper), double 5′ triphosphorylated dsRNA (middle), and the single 5′ triphosphorylated dsRNA (lower).

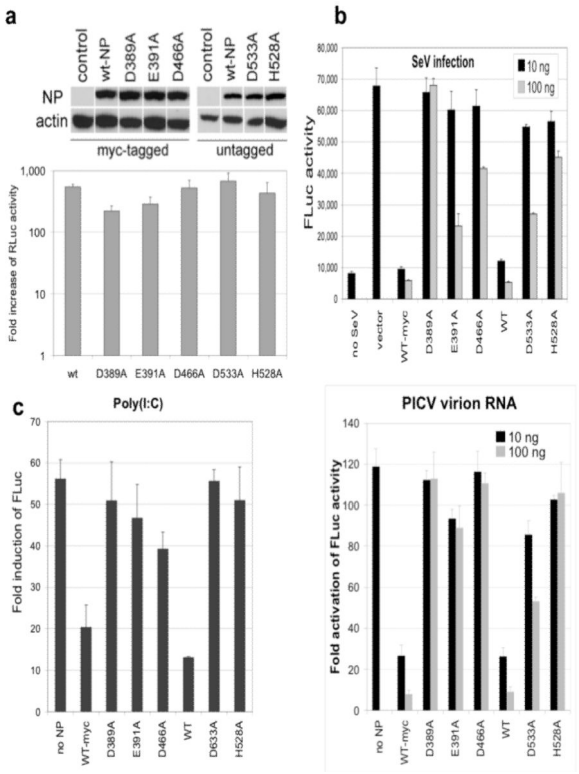

Figure 3. The exonuclease activity of NP is important for blocking the IFN induction

Results shown are the average (n=3) with error bars indicating the standard deviations. **a**, The NP catalytic mutants were expressed at similar levels to the WT in mammalian cells and had similar transcriptional activities in the LASV minigenome assay. **b**, The NP catalytic mutants were defective in suppressing the Sendai virus-induced IFN induction by a LUC-based IFNbeta promoter assay. **c**, The NP catalytic mutants were defective in suppressing the IFN production induced by the immunostimulatory RNAs, poly(I:C) and Pichinde virion-associated RNAs.

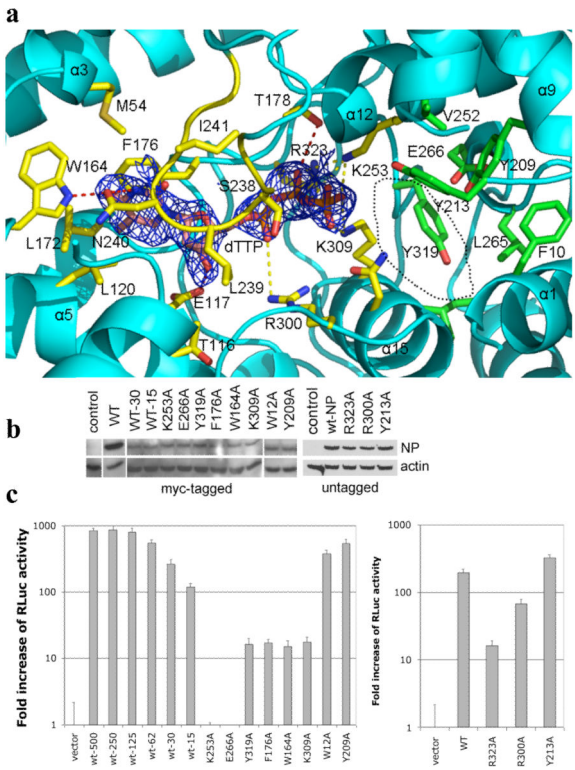

Figure 4. The cap-binding residues and their roles in viral RNA transcription

Results shown are the average (n=3) with error bars indicating the standard deviations. **a**, A cap analog dTTP is bound within the deep cavity of the N domain of LASV NP. Original Fo-Fc map for the dTTP in blue contoured 2.5 σ. The F176 and W164 or L172 (L120) residues form a typical cap-binding sandwich structure. The middle cavity binds the triphosphate moiety and the hydrophobic cavity entrance can accommodate the second base of the cap structure. **b**, The NP mutants were expressed at similar levels as the WT at 15 to 30 ng plasmid (WT-15, WT-30) in the transfected mammalian cells. **c**. Mutational analyses of the residues within the cap-binding cavity for the transcriptional activity using the LASV minigenome assay.